MACHINE BUILDING AND MACHINE SCIENCE

Check for updates

UDC 621.375. (075.8)
https://doi.org/10.23947/2687-1653-2022-22-2-150-160

Original article

Investigation of ACS Image Stabilization of On-board Optoelectronic Guidance and Tracking Devices

K. A. Burdinov ✉, K. M. Shashkina, Ehsan Shaghaei
Centre for Robotics and Mechatronics Components, Innopolis University, 1, Universitetskaya St., Innopolis, Russian Federation
✉sainquake@gmail.com

Abstract

Introduction. The movement of the carrier and external factors (the effects of the atmosphere, temperature and pressure) degrade significantly the image quality of the servo optoelectronic systems (OES) and the positioning accuracy of the emitting OES. The issues of image quality improvement and the probability of keeping the image of the observation object (OO) on the optical axis of the servo EOS are considered.

Materials and Methods. The development of an automatic control system for an optoelectronic device (ACS OED) involved solving a multi-criteria optimization problem taking into account a number of conflicting technical-and-economic (TE) requirements. The determination of tolerated dynamic errors (TDE) of image stabilization was a key issue in the development of on-board optoelectronic devices (OOED). Lagrange equations of the second kind and the mixed Gilbert method made it possible to obtain a mathematical model of the CO OED. Then, the decomposition of a two-link ACS with nonlinear cross-couplings in the CO was performed. A functional diagram of the image formation model of the OOED was presented. The parameters of the matrix photodetector and the requirements for the dynamic error of the ACS OED, taking into account the permissible MTF of the OED, were listed. The functions of transferring modulation, as well as linear, harmonic and vibrational shift of the image corresponding to the permissible and achieved TDE were visualized. Logarithmic frequency characteristics were created in the Mathcad environment. The two-link control system of the OED with the specified parameters of the CO for the considered movement was presented as two independent azimuth and elevation control channels.

Results. The processes of control of the on-board optoelectronic system in the stabilization and tracking modes were described. To study the dynamics of spatial control of the OOEP in accordance with the ACS methodology, a computer simulation model (CSM) of the digital automatic control systems (DACS) of the OED was developed. It was implemented in the Matlab environment and consisted of CSM CO, drives, proportional-integral-derivative (PID) controllers taking into account non-linearities, a central computing device (CCD), a guidance software device, a CSM-carrier that implemented the equations of motion. Harmonic vibrations of the carrier were described. The errors of tracking and stabilization in the tracking mode with an additional control action introduced in the form of a constant speed were determined. The dynamics of spatial control of the OOED was investigated. A computer simulation model of a digital automatic control system of an optoelectronic device, the results of modeling the DACS OED without considering the board movement, and the processes of OED control subject to movement were visualized.

Discussion and Conclusions. The stabilization accuracy was calculated for the studied cases. It was established that the stabilization tens of times exceeded the previously stated indicators, and it tens of times reduced the requirements for the convergence of the laser beam and the laser radiation power when developing the optical path of the product in

© Burdinov K. A., Shashkina K. M., Ehsan Shaghaei, 2022

question. The proposed CSM can be used in the development of the on-board optoelectronic systems. In this case, the application of the presented methodology and CSM will help to reduce labor costs and minimize errors.

Keywords: automatic control system, modulation-transfer function, servo system, optimization, optoelectronic device.

Acknowledgements: the authors would like to thank the management of the NTI Competence Center program "Technologies in Robotics and Mechatronics Components" for their assistance in preparing this article.

For citation: K. A. Burdinov, K. M. Shashkina, Ehsan Shaghaei. Investigation of ACS image stabilization of on-board optoelectronic guidance and tracking devices. Advanced Engineering Research, 2022, vol. 22, no. 2, pp. 150–160. https://doi.org/10.23947/2687-1653-2022-22-2-150-160

Introduction. When designing modern on-board optoelectronic devices (OED) and complexes, methods of computer modeling of optoelectronic systems (OES) are widely used. Such authors as Yu. G. Yakushenkov, V. V. Tarasov, I. P. Torshina, V. P. Ivanov, V. A. Baloev, V. A. Ovsyannikov, V. L. Filippov, worked on these tasks. Computer modeling enables to solve the problems of rational choice of the structure, parameters, and element base of the OES, providing the required performance indicators under specified constraints without expensive field studies and tests.

The movement of the carrier and external factors (temperature, pressure) degrade significantly the image quality of the servo OES and the positioning accuracy of the emitting OES. The probability of holding the image of the object of observation (OO) on the optical axis of the tracking OES is reduced. For emitting OES, the positioning accuracy and the probability of performing observation tasks are reduced. To hold the image in vision or in the irradiation sector, it is required to capture a fairly large solid viewing angle. Hence, it is required to increase the dimensions of optical systems and power electronics capacities. To avoid this, controlled radiating OES is used. The above-mentioned features of the OED limit the development of the ACS OED. This problem was considered by V. A. Strezhnev, V. M. Matrosov, A. S. Zemlyakov, N. N. Malivanov, E. I. Somov, A. I. Malikov, V. A. Krenev, A. I. Karpov, D. A. Molin, A. V. Mikhalitsyn. When designing controlled OED operating in guidance and tracking modes, the following fact was established: the guidance time and the accuracy of stabilization of the optical axis, as well as the dynamics of the OED subsystems affect significantly the image quality.

Thus, the task of minimizing the time and increasing the accuracy of pointing and holding the image of the OO in vision of the controlled OED is a challenge. In this regard, the following is required:

− development of mathematical models of power lines as control objects;

− synthesis of control algorithms;

− creation of computer simulation models (CSM);

− study on control systems that take into account the dynamics of the movement of a controlled OED;

− determination of parameters affecting the dynamic properties and image quality.

The work aimed at improving the accuracy characteristics and image quality of OED operating in the guidance, stabilization and tracking modes, due to the rational choice of their parameters during synthesis and modeling.

Materials and Methods. The development of ACS OED started with solving a multi-criteria optimization problem that took into account conflicting technical-and-economic (TE) requirements. In the development of study [1], a modified method of designing a self-propelled ACS OED was proposed. For the quality criterion of the ACS, we took a set of dynamic characteristics of control channels that met the conditions:

$$T_{\text{оэп}}(\nu_{\text{н}}) \geq T_{\text{оэп}}^{\text{доп}}(\nu_{\text{н}}), \delta(\omega) \leq \delta^{\text{доп}}(\omega), \Delta\alpha_{\text{к}} \leq \Delta\alpha_{\text{к}}^{\text{доп}}, \Delta\dot{\alpha}_{\text{к}} \leq \Delta\dot{\alpha}_{\text{к}}^{\text{доп}}, \quad (1)$$
$$M \leq M^{\text{доп}}, |\Delta\varphi| \geq \Delta\varphi^{\text{доп}}, |\Delta L| \geq \Delta L^{\text{доп}}.$$

Here, $T_{\text{оэп}}^{\text{доп}}(\nu_{\text{н}}), T_{\text{оэп}}(\nu_{\text{н}})$ — permissible and implemented modulation-transfer function (MTF) of the OED at the Nyquist frequency, $\delta(\omega)$; $\delta^{\text{доп}}$ — amplitude frequency response of cross-couplings and its acceptable decomposition value; $\Delta\alpha_{\text{к}}^{\text{доп}}, \Delta\dot{\alpha}_{\text{к}}^{\text{доп}}, \Delta\alpha_{\text{к}}, \Delta\dot{\alpha}_{\text{к}}$ — permissible and steady-state values of the dynamic errors of the ACS in angle and angular velocity under the action of disturbances under conditions close to the actual operation of the ACS; $\kappa = 1, 2, \ldots$ — number of the control channel providing image quality; $M_{\text{доп}} = 1.05–1.25$ — oscillation index, $\Delta\varphi$; ΔL — stability margins in phase and amplitude.

The key issue in the development of the OED is the determination of tolerated dynamic errors (TDE) of image stabilization.

The image formation scheme of the on-board optoelectronic device (OOED) is shown in Figure 1.

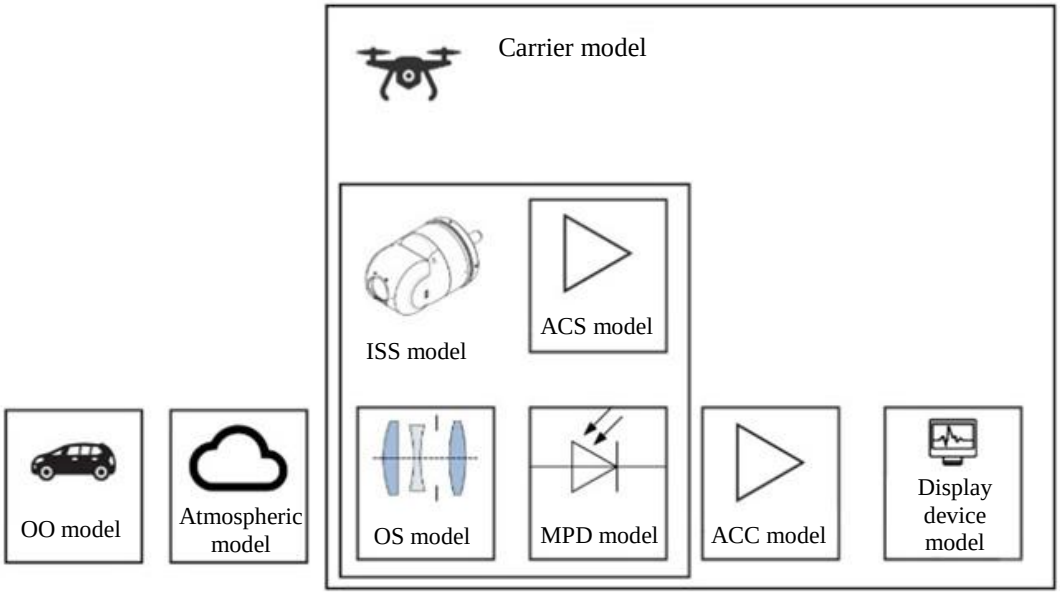

Fig. 1. Functional diagram of the OOED imaging model: OO — object of observation; OS — optical system; MPD — matrix photodetector; ACD — amplifying-converting device; ISS — image stabilization system

The MTF OOED should meet the condition that provides acceptable image quality [2]:

$$T_{\text{ОЭС}}(\nu) = T_{\text{ат}}(\nu)T_{\text{об}}(\nu)T_{\text{фп}}(\nu)T_{\text{упу}}(\nu)T_{\text{ССИ}}(\nu) > T_{\text{ОЭС}}^{\text{доп}}(\nu), \quad (2)$$

$$T_{\text{ОЭС}}^{\text{доп}}(\nu) = 2\left(Sinc\left(N\frac{\gamma_{\text{и}}}{2}\right)\right)^{-1} exp\left[-\frac{\left(N\gamma_{\text{р}}\right)^2}{16\,ln(2m)}\right].$$

Here, $T_{\text{ОЭС}}(\nu)$ — MTF OED; N — spatial frequency; $T_{\text{ОЭС}}^{\text{доп}}(\nu)$ — admissible MTF OOED; $T_{\text{ат}}(\nu)$ — atmospheric MTF; $T_{\text{об}}(\nu)$ — lens MTF; $T_{\text{фп}}(\nu)$ —photodetector MTF; $T_{\text{упу}}(\nu)$ — optical information conversion function MTF [1]; $T_{\text{ССИ}}(\nu)$ — MTF of the image shift (dynamic error of the ISS), depending on the type of dynamic displacement of the image: linear (Л) — $x(t) = Vt$, harmonic (Г) — $x(t) = a_0 sin(t)$, random (R), and defocusing.

The permissible MTF of the image stabilization system includes tracking, stabilization, vibration protection (VPS) and automatic focusing (AFS) systems [3]:

$$T_{\text{ССИ}}(N) = T_{\text{Л}}(N)T_{\text{Г}}(N)T_{\text{В}}(N)T_{\Phi}(N) \geq T_{\text{ССИ}}^{\text{доп}}(N) = \frac{T_{\text{оэп}}^{\text{доп}}(N)}{T_{\text{ст}}(\text{N})},$$

$$T_{\text{Л}}(\nu) = sinc(\pi\Delta\alpha_{\text{Л}}\nu), T_{\text{Г}}(\nu) = J_0(2\pi\Delta\alpha_{0\text{Г}}\nu), T_{\text{В}}(\nu) = exp[-2(\pi\Delta\alpha_{\text{В}}\nu)^2], \quad (3)$$

$$T_{\Phi}(\nu) = \frac{2J_1(\Delta_{\phi})}{\Delta_{\phi}}, \Delta_{\phi} = 28\pi\sigma\left(\frac{\lambda_{\text{ср}}\nu}{D}\right)\left(1 - \frac{\lambda_{\text{ср}}\nu}{D}\right),$$

$$T_{\text{ст}}(N) = T_{\text{ат}}(N)T_{\text{об}}(N)T_{\text{фп}}(N)T_{\text{упу}}(N).$$

Here, $T_{\text{Л}}(N)$ — image linear shift error; $T_{\text{Г}}(N)$ — sinusoidal error amplitude; $T_{\text{В}}(N)$ — average value of vibration amplitude error; J_0 — zero-order Bessel function of the first kind; $J_1(\Delta_{\phi})$ — Bessel function of the first kind of the first order; Δ_{ϕ} — focus error (mm); σ — average value of wave aberration in fractions of a wavelength; $\lambda_{\text{ср}}$ — average wavelength of the spectral range.

Let us assume that each subsystem of the ACS must make the same amount of change in the image quality of the OED and $T_{\text{ст}}(N)$ = const during observation. Then, the definition of acceptable MTF R, VPS, AFS, will be simplified (3):

$$T_j^{\text{доп}}(\nu) = \sqrt[4]{\frac{T_{\text{ОЭС}}^{\text{доп}}(\nu)}{T_{\text{ст}}(\nu)}} \quad (j = \text{Л}, \Gamma, \text{В}, \Phi). \quad (4)$$

We expand functions $T_{\text{Л}}(N), T_{\Gamma}(N), T_B(N), T_{\Phi}(N)$ (3) into a series and obtain expressions that determine the TDE:

$$\Delta\alpha_{Л}^{доп} \leq \frac{0{,}824\sqrt{1-T_{Л}^{доп}(\nu_н)}}{\nu_н}, \Delta\alpha_{Г}^{доп} \leq= \frac{0{,}335\sqrt{1-T_{Г}^{доп}(\nu_н)}}{\nu_н}, \quad (5)$$

$$\Delta_{Ф}^{доп} \leq 3{,}018\sqrt{1-T_{Ф}^{доп}(\nu_н)}, \Delta\alpha_{В}^{доп} \leq \frac{\sqrt{0.5\,ln[T_{В}^{доп}(\nu_н)]^{-1}}}{\pi\nu_н}.$$

Here, $\nu_н$ — Nyquist frequency.

The limiting spatial frequency that the OED should resolve during the observation process is determined by the Johnson criterion:

$$\nu_{пр} = \frac{N_Д L}{h_{кр}}, \nu_н = 0{,}5\nu_{пр}, \quad (6)$$

where $\nu_{пр}$ — angular (bar/rad) limiting spatial frequency; $N_Д$ — number of resolution elements (Johnson numbers); L — distance to OO; $h_{кр}$ — critical size of OO.

When decomposing, all members of the series are discarded, except the first ones, therefore, the tolerances obtained should be revised by gradient descent.

The above reasoning allowed us to determine the accuracy of image stabilization of the onboard optoelectronic system (OOES) for tracking and stabilization modes. A methodology and a program for calculating MTF and tolerances were developed (Patent RU2021660340[1]).

Let us denote requirements for the dynamic error of the ACS OED, taking into account the permissible MTF OED. Initial data for calculation:

− diameter of the entrance pupil — D = 90 mm,

− OS focal length — f`= 100 mm,

− wavelength — λ = 4 μm,

− distance to the object of observation — L = 10 km,

− meteorological visibility — SM = 15 km,

− flight altitude — H = 5 km,

− number of MPD elements — 256×256,

− frame rate — F = 400 Hz,

− probability of correct detection — $P_{обн}$ = 0.8,

− false alarm probability — $P_{лт} = 10^{-4}$,

− signal-to-noise ratio of the amplifier — optimal filter — m = 1.105,

− angular size of the object of observation — $\gamma_s = 5\cdot10^{-5}$ rad,

− angular distance between two adjacent targets — $\gamma_р = 3.34\cdot10^{-3}$ rad.

MPD parameters:

− d = 0. 0.25a — thickness of the photosensitive layer,

− $\varepsilon_n = 4\cdot10^{-5}$ — charge transfer inefficiency,

− α_c = 2 — number of samples per 1 element,

− $k_з$ = 0.6 — fill factor,

− $\tau = 5.4\cdot10^{-9}$ s — reading time,

− $\tau_{пр} = 5\cdot10^{-10}$s — time constant of the transducer.

Figure 2 shows the MTF of linear, harmonic and vibrational shift of the image corresponding to the permissible and obtained DDP of the ACS OOED.

[1] Program for calculating the modulation transfer function of an optoelectronic device based on UAV: RF patent 2021660340, 2021. Innopolis University. (In Russ.)

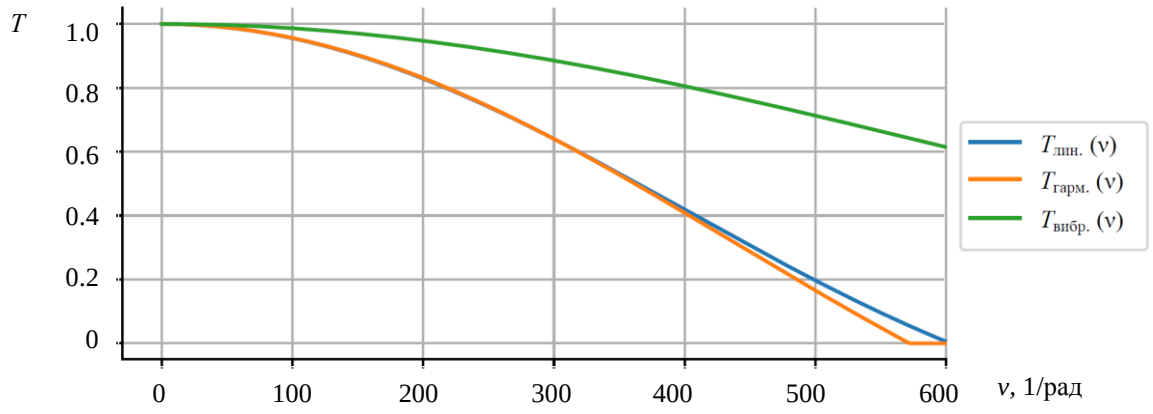

Fig. 2. Modulation transfer functions $T_j^{доп}(\nu)$

In accordance with (3)–(5) and the initial data for the calculation, we determined: $\nu_{пр} = 600$ rad^{-1} of the OOED observation channel in the infrared region with a detection probability of $P = 0.8$. For MTF OOED and TDE ACS: $\Delta\alpha_Л = 3.5$ ang. min, $\Delta\alpha_Г = 3.1$ ang. min, $\Delta\alpha_В = 3.0$ ang. min.

On the basis of the Lagrange equations of the second kind and the mixed Gilbert method, a mathematical model of the SO OED [4] of guidance and tracking was obtained in the form of three information channels driven by DBM electric motors along the gimbal axles. We presented it in a matrix form[2]:

$$A(q)\ddot{q} + B(t,q)\dot{q} + F(q,\dot{q}) + W(t,q) + Q(t,q) = M_{дв} - M_{тр}. \quad (7)$$

Here, $q = (\alpha \quad \beta)^T$, α, β — CO rotation angles in azimuth and elevation..

$$A(q) = \begin{pmatrix} B_1 + B(\beta) & -D(\beta) \\ -D(\beta) & C_2 \end{pmatrix}, B(t,q) = \begin{pmatrix} 0 & b_{\alpha\beta}(t,\alpha,\beta) \\ -b_{\alpha\beta}(t,\alpha,\beta) & 0 \end{pmatrix},$$

$$F(q,\dot{q}) = \begin{pmatrix} -2\dot{\alpha}\dot{\beta}F(\alpha,\beta) - \dot{\beta}^2E(\beta) \\ \dot{\alpha}^2F(\beta) \end{pmatrix}, W(t,q) = \begin{pmatrix} w_\alpha(t,q) \\ w_\beta(t,q) \end{pmatrix},$$

$$Q(t,q) = \begin{pmatrix} r_\alpha(q) \\ r_\beta(q) \end{pmatrix}\left(\tilde{a}_O(t) + A_y A_\tau \tilde{g}\right), M_{дв} = \begin{pmatrix} M_{дв.1} \\ M_{дв.2} \end{pmatrix}, M_{тр} = \begin{pmatrix} M_{тр.1}sign(\dot{\alpha}) \\ M_{тр.2}sign(\dot{\beta}) \end{pmatrix},$$

$$b_{\alpha\beta}(t,\alpha,\beta) = \{(2A_2(\beta) - C_2)\cos\alpha - 2E(\beta)\sin\alpha\}\omega_{x_y}(t) - 2F(\beta)\omega_{y_y}(t) - \{(2A_2(\beta) - C_2)\sin\alpha + 2E(\beta)\cos\alpha\}\omega_{z_y}(t),$$

$$w_\alpha(t,q) = \left\{-\dot{\omega}_{x_y}(t)F(\alpha,\beta) + \dot{\omega}_{y_y}(t)\left(B_1 + B(\beta)\right) - \dot{\omega}_{z_y}(t)D(\alpha,\beta)\right\} + \left\{E(\alpha,\beta)\Omega_{x_y}^2(t) - E(\alpha,\beta)\omega_{z_y}^2(t) + D(\alpha,\beta)\omega(t)\omega_{y_y}(t) + 2A_1(\alpha,\beta)\omega_{x_y}(t)\omega_{z_y}(t) - F(\alpha,\beta)\omega_{y_y}(t)\omega_{z_y}(t)\right\},$$

$$w_\beta(t,q) = \left\{-\dot{\omega}_{x_y}(t)[E(\beta)\cos(\alpha) - C_2\sin(\alpha)] - \dot{\omega}_{y_y}(t)D(\beta) + \dot{\omega}_{z_y}(t)[E(\beta)\sin(\alpha) + C_2\cos(\alpha)]\right\} - \frac{1}{2}\left\{[F(\beta)(1+\cos(2\alpha)) + D(\beta)\sin(2\alpha)]\omega_{x_y}^2(t) - 2F(\beta)\omega_{y_y}^2(t) + [F(\beta)(1-\cos(2\alpha)) - D(\beta)\sin(2\alpha)]\omega_{z_y}^2(t) + 2[2A_2(\beta)\cos(\alpha) - E(\beta)\sin(\alpha)]\omega_{x_y}(t)\omega_{y_y}(t) - 2[F(\beta)\sin(2\alpha) - D(\beta)\cos(2\alpha)]\omega_{x_y}(t)\omega_{z_y}(t) - 2[E(\beta)\cos(\alpha) + 2A_2(\beta)\sin(\alpha)]\omega_{y_y}(t)\omega_{z_y}(t)\right\},$$

$$r_\alpha(q) = m_1\begin{pmatrix} -x_{C_1}\sin(\alpha) + z_{C_1}\cos(\alpha) \\ 0 \\ -x_{C_1}\cos(\alpha) - z_{C_1}\sin(\alpha) \end{pmatrix}^T + m_2\begin{pmatrix} -\left(x_{C_2}\cos(\beta) - y_{C_2}\sin(\beta)\right)\sin(\alpha) + z_{C_2}\cos(\alpha) \\ 0 \\ -\left(x_{C_2}\cos(\beta) - y_{C_2}\sin(\beta)\right)\cos(\alpha) - z_{C_2}\sin(\alpha) \end{pmatrix}^T,$$

http://vestnik-donstu.ru

[2]Burdinov KA, et al. Matematicheskaya model' i sintez sistemy avtomaticheskogo upravleniya bortovogo optiko-ehlektronnogo pribora. In: Proc. XII All-Russian Congress on Fundamental Problems of Theoretical and Applied Mechanics, Ufa, 2019. P. 190–192. (In Russ.)

$$r_\beta(q) = m_2 \begin{pmatrix} \left(-x_{C_2}\, sin(\beta) - y_{C_2}\, cos(\beta)\right) cos(\alpha) \\ x_{C_2}\, cos(\beta) - y_{C_2}\, sin(\beta) \\ \left(x_{C_2}\, sin(\beta) + y_{C_2}\, cos(\beta)\right) sin(\alpha) \end{pmatrix}^T.$$

The next stage of development was the decomposition of doubly connected ACS [5] with nonlinear cross couplings in the CO, which is the studied OED. The linearized equations of motion with respect to the trajectory have the form:

$$a \times_{\text{вх}} (t) = \dot{\alpha}_0 t \in 0 \div 2\pi; \beta \times_{\text{вх}} (t), = \dot{\beta}_0 t \in 0 \div \pi/2,$$

$$\begin{aligned} &(a_{10} + a_{11})\Delta\ddot{\alpha} + (b_{10} + b_{11})\Delta\dot{\alpha} + c_{11}\Delta\alpha + a_{12}\Delta\ddot{\beta} + b_{12}\Delta\dot{\beta} + c_{12}\Delta\beta = K_{u1}\Delta u_1, \\ &a_{21}\Delta\ddot{\alpha} + b_{21}\Delta\dot{\alpha} + a_{20}\Delta\ddot{\beta} + b_{20}\Delta\dot{\beta} + c_{22}\Delta\beta = K_{u2}\Delta u_2, \\ &\Delta u_1 = R_1(p)\Delta\varepsilon_1, \Delta\varepsilon_1 = \Delta\alpha^*_{\text{вх}} - \Delta\alpha^*; \Delta u_2 = R_2(p)\Delta\varepsilon_2, \Delta\varepsilon_2 = \Delta\beta^*_{\text{вх}} - \Delta\beta^*. \end{aligned} \quad (8)$$

Having constructed the variable coefficients of system (8), we determine their values at $t = t_к^*$ at "dangerous" points at which the parameters change significantly or change signs in the range of angles ($\beta^* = 0 \div \pi/2$, $\alpha^* = 0 \div 2\pi$). Then, reducing system (8) (for $t = t_к^*$) to a system with constant parameters and using Cramer's rule, we express it in the form of transfer functions (TF) at points $t = t_к^*$:

$$\Delta\alpha = W_{11}(p, t_к^*)\Delta u_1 - W_{12}(p, t_к^*)\Delta u_2, \quad (9)$$

$$\Delta\beta = W_{22}(p, t_к^*)\Delta u_2 - W_{21}(p, t_к^*)\Delta u_1.$$

The obtained TF (9) taking into account (8) for each selected moment of time ($t = t_к^*$) can be presented in the form of a block diagram with direct cross couplings (CC, Fig. 3). From now on, for simplicity of writing, we denote TF as $W_{кij}(p) = W_{ij}(p, t_к^*)$.

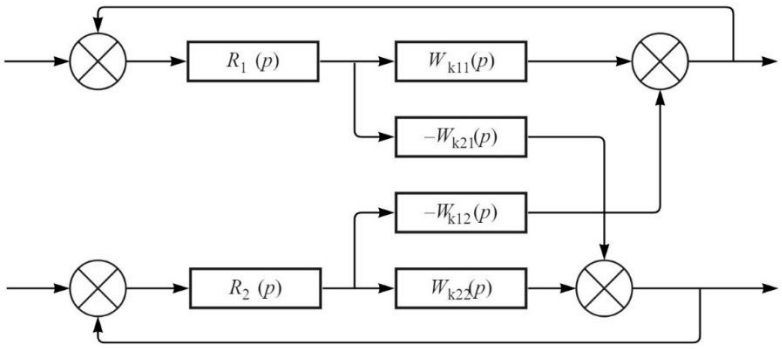

Fig. 3. Structural diagram of doubly connected ACS

We evaluate the CC ACS by their frequency response (FR). For this purpose, we write down the TF of the open system, taking into account the 2nd closed control channel when $\Delta\beta_{\text{вх}} = 0$ (Fig. 4).

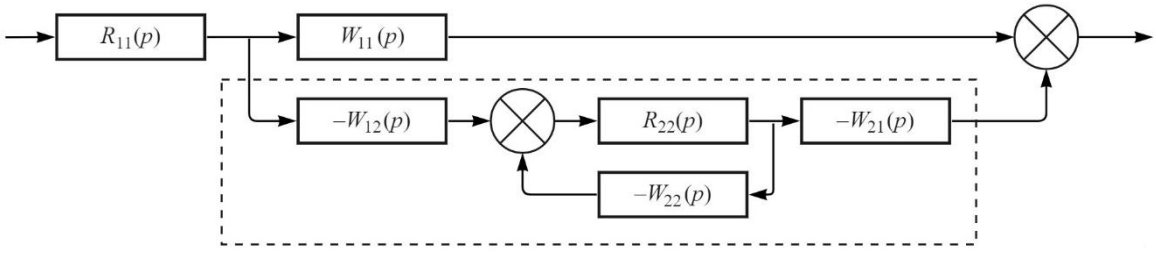

Fig. 4. Structural diagram of ACS, open on one control channel

Let us build hodograph $W_{к1}^{\text{раз}}(j\omega) = R_1(j\omega)W_{к11}(j\omega)$ and tubes around it with radii for each moment of time $t_к^*$:

$$\varepsilon_{1к}(\omega) = R_1(\omega)\, W_{к11}(\omega)\, W_{2к}(\omega)\, \delta_к(\omega). \quad (10)$$

Taking into account (10) and the Nyquist criterion, it is possible to judge the stability of the ACS (1), (2) and the influence of the CC on its stability in the range of scanning angles (3).

As a result, for each ($t_к^*$-th), we determine the CC time:

$$\delta_{\kappa i}(\omega) = \delta_{\kappa 12}(\omega)\delta_{\kappa 21}(\omega)W_{\kappa j}(\omega) = \frac{W_{\kappa 12}(\omega)}{W_{\kappa 11}(\omega)}\frac{W_{\kappa 21}(\omega)}{W_{\kappa 22}(\omega)}W_{\kappa j}(\omega), (i,j = 1,2). \quad (11)$$

Let us consider the CC ACS that satisfy the decomposition conditions.

According to (8), (11), from the CO mass geometry data, for 11 selected points in time, we determined ($t_к^*$ = 0; 0.89; 1.35; 1.58; 1.71; 2.3; 2.97; 3.8; 4.5; 4.75; 6.28 s). We built $a_{ij}(t)$, $b_{ij}(t)$, $c_{ij}(t)$. Logarithmic frequency response (LFR) $\delta_к(\omega)$ (k = 1.11) was created in the Mathcad environment (Fig. 5).

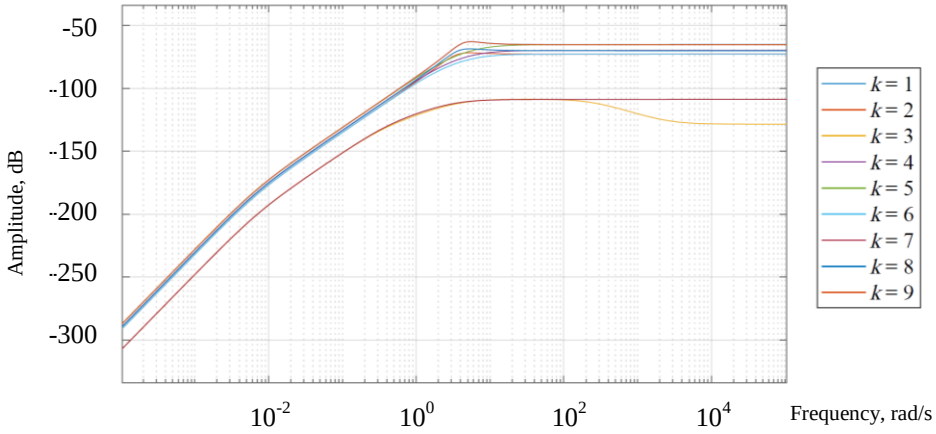

Fig. 5. Logarithmic frequency response $\delta_к(\omega)$

Figure 5 shows that the entire LFR set does not exceed –50 dB. From the analysis of LFR $\delta_к(\omega)$, we have the results presented below.

$\forall\omega\in\Omega_1 = (10^{-4}\div10^4)$ rad/s.

The following was determined: max $\delta_к(\omega)$ = 0.0136 (–37.3 dB) < $\delta^{доп}$ = 0.0335 (–29.5 dB), $\Delta L = M^{доп} / (M^{доп} + 1)$ = 0.535 (–5.43 dB) at $M_{10} = M_{20}$ = 1.1; $M^{доп}$ = 1.15.

Hence, a doubly connected control system (8) of the OED with the given parameters of the CO for the motion in question can be presented as two independent control channels in azimuth and elevation angle.

Research Results. Figures 6 and 7 show the OOED control processes in stabilization and tracking modes. The scale of the misalignment graphs has been increased by 600 times. The graphs of the program control and the output values visually coincide.

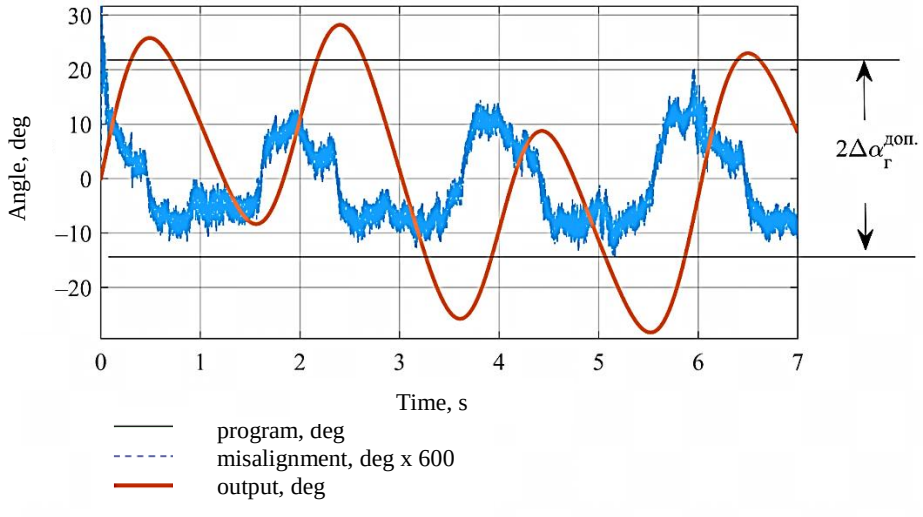

Fig. 6. OOED stabilization processes in azimuth

http://vestnik-donstu.ru

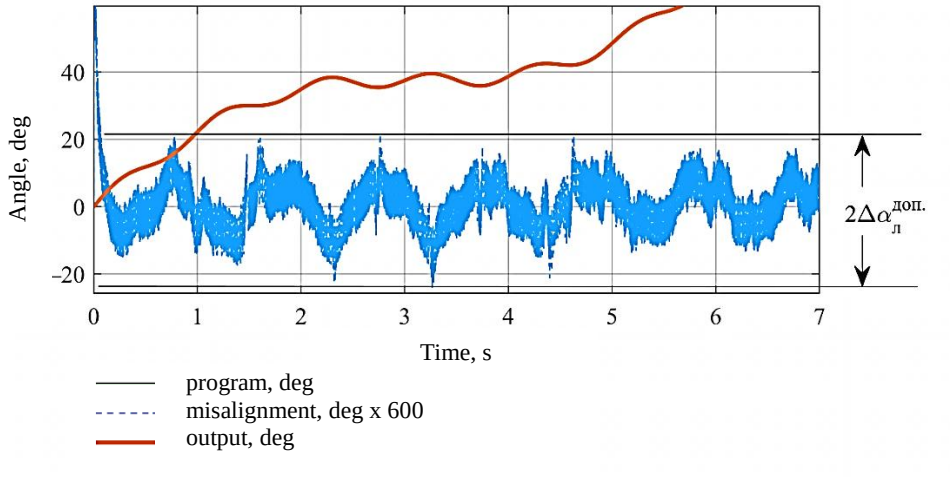

Fig. 7. OOED tracking processes in azimuth

We describe the harmonic oscillations of the carrier: $A_1 = A_2 = 2^0$ (amplitudes), $T_1 = T_2 = 1$ s (oscillation periods), and $A_1 = A_2 = 12^0$, $T_1 = T_2 = 6.28$ s. We indicate the load moments: $M_{дв1} = 2.2$ Nm, $M_{дв1} = 0.3$ Nm. With such harmonic oscillations and load moments, the error of stabilization of the sighting axis does not exceed:

− in azimuth — 1.2 ang. min,

− in elevation angle — 1.6 ang. min.

In tracking mode, with an additional control action introduced in the form of a constant speed of 12 ^{deg}/s, the error of tracking and stabilization does not exceed 1.7 ang. min in azimuth and 1.3 ang. min in elevation angle.

To study the dynamics of the spatial control of the OOED in accordance with the ACS technique, the CSM of the digital automatic control system (DACS) of a specific OED was developed (Fig. 8) [1].

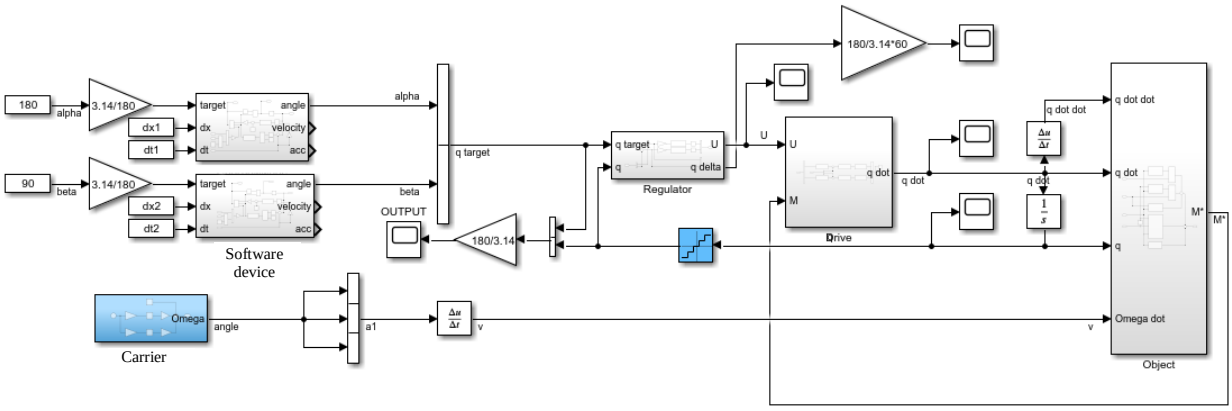

Fig. 8. Computer simulation model of a digital system for automatic control of an optoelectronic device

The solution is implemented in the Matlab Simulink environment. Its elements:

− CSM CO (Object) obtained according to (7);

− CSM of drives (Drive);

− CSM of PID-regulators (Regulator) taking into account non-linearities and DCD;

− CSM of software guidance device;

− Carrier CSM that implements the equations of carrier motion.

Figures 6 and 7 show the results of modeling the DACS OED without taking into account the movement of the board. In this case:

− guidance error does not exceed 18 ang. min in azimuth, 10 ang. min in elevation angle;

− tracking error — 0.6 ang. min in azimuth, 0.6 ang. min in elevation angle;

− stabilization error — 0.45 ang. min in azimuth, 0.6 ang. min in elevation angle.

Figure 9 shows the control processes of the OED, taking into account its movement. The azimuth guidance error is 2 ang. min, the elevation angle error is 5 ang. min. The error of tracking and stabilization is 0.8 ang. min in azimuth, 1.3 ang. min in elevation angle.

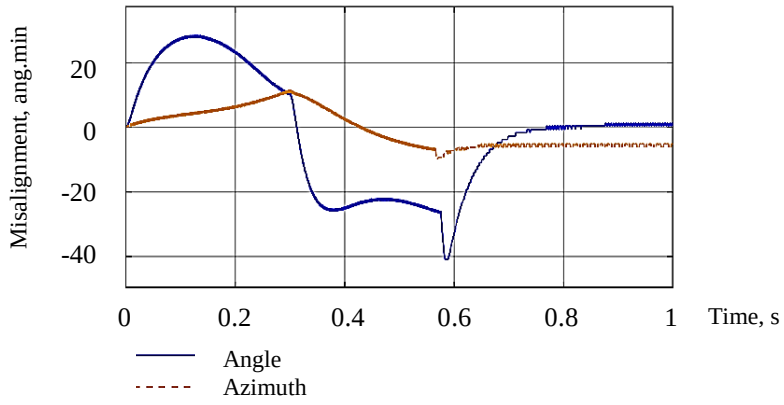

a)

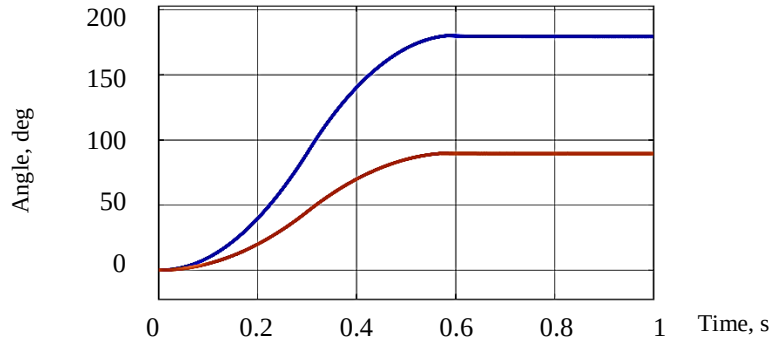

b)

Fig. 9. Simulation results of the system in two-channel guidance mode (degrees):
a — system misalignment; *b* — transient schedules. In second case, schedules of program control (alpha target, beta target) and output value (alpha, beta) visually coincide

Discussion and Conclusions. The results obtained are presented below.

1. A technique for evaluating tolerances for the accuracy of image stabilization of the OOED under conditions of controlled and temperature influences was proposed. (Patent RU2021660340). Analytical estimates of the TDE image stabilization according to (4), (5) for tracking and stabilization modes based on the MTF OED were presented. The requirements for the ACS were obtained, providing a solution to the problem of detecting OO in the infrared region.

2. The decomposition acceptance criterion was given, the method of decomposition of a doubly connected ACS OEP with the use of computer technologies was described. The requirements for the design parameters of the CO of a real device were defined. That allowed synthesizing the ACS OEP as two independent control channels.

3. The CSM ACS OED was proposed to study the dynamics of isolated control channels and spatial control. In this case, the nonlinearity and non-stationarity of a specific CO were taken into account.

4. A mechanical model of the OED was developed, the equations of the dynamics of spatial motion (7) of the CO were obtained.

5. The parameters of the PID-controllers were synthesized, providing stable guidance and stabilization of the OED under all specified modes. Q-factor in speed: $K_{v1} = (3700 \div 4000)s^{-1}, K_{v2} = (3000 \div 3300)\, s^{-1}$. Corrective links: $T_{к11} = T_{к12} = 0.05s, T_{к21} = T_{к22} = 5 \times 10^{-5}\, s$. This provided more accurate operation of the flight planning system and trajectory construction [6–8].

6. It was shown that with the help of CSM, it was possible to obtain the required time and error of guidance, stabilization, and tracking. In this case, the guidance speed was 0.6 s. The corresponding indicator of foreign analogues — 1 s[3].

7. In [9], a laser counteraction system was considered. Its technical characteristics allowed performing the task at W = 1000 W/steradian and laser power P = 3.1 W. It was shown in [10] that the required radiation power was W = 2700 W/steradian at a laser power of P = 200 MW.

http://vestnik-donstu.ru

[3] Directed Infrared Countermeasure (DIRCM). EMSOPEDIA. emsopedia.org . URL: https://www.emsopedia.org/entries/directed-infrared-countermeasure-dircm/ (accessed: 01.05.2022).

We calculated the required stabilization accuracy for each of the presented cases using formula $\Delta = \frac{2\times180\times60}{\pi}\arccos\left(1-\frac{P}{2\,\pi\,W}\right)$ [ang. min] and made Table 1.

Table 1

Comparison of required stabilization accuracy

	Radiation power (*W*), W/sterad	Laser power (*P*), W	Required stabilization accuracy (Δ), ang.min
Installation [11]	2,700	0.2	33.4
Installation [10]	1,000	3.1	216.1
Product			1.3

Thus, the accuracy of stabilization of the proposed system was ten times higher than that required in papers [9, 10]. And this reduces the requirements for the convergence of the laser beam and the laser radiation power tenfold when developing the optical path of the product in question.

List of abbreviations and conventions

OES — optoelectronic system,
OED — optoelectronic device,
OO — object of observation,
CSM — computer simulation model,
ACS — automatic control system,
MTF — modulation transfer function,
TDE — tolerated dynamic error,
ISS — image stabilization system,
MPD — matrix photodetector.

References

1. Baloev VA, Burdinov KA, Karpov AI, et al. Technique for developing and testing the control and vibration-proofing systems of on-board optoelectronic devices. Journal of Optical Technology. 2021;88:24–36. https://doi.org/10.17586/1023-5086-2021-88-03-24-36

2. Molin DA. Use of the modulation transfer function for assessment of admissible characteristics of optoelectronic devices. Vestnik of KNRTU n.a. A. N. Tupolev. 2011;1:68–75.

3. Sokolskiy MN. Dopuski i kachestvo opticheskogo izobrazheniya. Leningrad: Mashinostroenie; 1989. 220 p. (In Russ.)

4. Baloev VA, Karpov AI, Krenev VA, et al. Imitatsionnoe modelirovanie dvukhstupenchatoi sistemy upravleniya skaniruyushchim ustroistvom bortovogo bazirovaniya. Journal of Optical Technology. 2017;84:6–14. (In Russ.)

5. Garkushenko VI. On synthesizing of multiply connected non-stationary system of control in the presence of incomplete information. Vestnik of KNRTU n.a. A. N. Tupolev. 2003;3:47–49.

6. Bangura M, Mahony R. Real-time model predictive control for quadrotors. IFAC Proceedings Volumes. 2014;47:11773–11780 https://doi.org/10.3182/20140824-6-ZA-1003.00203

7. Geesara Kulathunga, Fedorenko R, Kopylov S, et al. Real-time long range trajectory replanning for MAVs in the presence of dynamic obstacles. URL: https://ieeexplore.ieee.org/document/9162605 (accessed: 13.06.2022) https://doi.org/10.1109/ACIRS49895.2020.9162605

8. Geesara Prathap Kulathunga, Hany Hamed, Devitt D, et al. Optimization-Based Trajectory Tracking Approach for Multi-Rotor Aerial Vehicles in Unknown Environments. IEEE Robotics and Automation Letters. 2022;7:4598–4605.

9. HHPTh Bekman, JC van den Heuvel, FJM van Putten, et al. Development of a mid-infrared laser for study of infrared countermeasures techniques. URL: https://www.spiedigitallibrary.org/conference-proceedings-of-spie/5615/0000/Development-of-a-mid-infrared-laser-for-study-of-infrared/10.1117/12.578214.short?SSO=1 (accessed: 13.06.2022) https://doi.org/10.1117/12.578214

10. Toet A, Benoist KW, JNJ van Lingen, et al. Optical countermeasures against CLOS weapon systems. URL: https://www.spiedigitallibrary.org/conference-proceedings-of-spie/8898/1/Optical-countermeasures-against-CLOS-weapon-systems/10.1117/12.2028342.short (accessed: 13.06.2022) http://dx.doi.org/10.1117/12.2028342

Received 05.05.2022
Revised 02.06.2022
Accepted 02.06.2022

About the Authors:

Burdinov, Konstantin A., senior engineer, Center for Technologies in Robotics and Mechatronics Components, Innopolis University (1, Universitetskaya St., Innopolis, 420500, RF), ResearcherID, ORCID, sainquake@gmail.com

Shashkina, Kseniya M., Head of the Laboratory of Unmanned Technology Innopolis University (1, Universitetskaya St., Innopolis, 420500, RF), ScopusID, ORCID, k.shashkina@innopolis.ru

Ehsan Shaghaei, engineer, Center for Technologies in Robotics and Mechatronics Components, Innopolis University (1, Universitetskaya St., Innopolis, 420500, RF), ResearcherID, ScopusID, ORCID, e.shaghaei@innopolis.university

Claimed contributorship

K. A. Burdinov: academic advising; development of the methodology; analysis of the research results; the text revision; correction of the conclusions. Ehsan Shaghaei: computational analysis; text preparation; formulation of conclusions. K. M. Shashkina: proofreading and revision of the text.

Conflict of interest statement

The authors do not have any conflict of interest.

All authors have read and approved the final manuscript.